**We thank you very much for reading the manuscript and providing very helpful and constructive comments.**

# Reviewer #1

## General Comments

1. **I would recommend shortening the abstract. About 60% of it is introductory information and could be reduced to a couple of sentences. The abstract should be a "brief introduction of the topic". Also the abstract should include some specific results and should "mentions possible directions for prospective research."**

   **Response:** We shortened the abstract to make it as concise as possible. Please see the new abstract in the manuscript.

2. **My largest issue is the paper needs to thorough rewrite; not for technical reasons as much as the English is poor. This gets increasingly apparent after the introduction. It is filled with colloquial language, "we" and "us", and an excessive amount of connective words like "Besides", "Nevertheless", "furthermore", "consequently", "in principle", "however", "hence", "again and again", "on the other hand". On many occasions I had to guess the interpretation of a sentence and it is difficult to follow the idea being developed in many paragraphs.**

   **Response:** Thank you for the advice. We tried to remove some unnecessary linking works to make the manuscript easier to understand.

3. **The conclusion were adequate but I would request further information in a couple of areas that would help the reader accept these conclusions. Unfortunately I may have missed this due to General comment 2.**

   (a) **I felt section 3.2 requires further information i. Where is the battery, ESCs, and other equipment located? Could this be incorporated into a Figure (Figure 3?) or added as a separate figure?**

   **Response:** We included a figure that shows the mentioned components in the manuscript.

   (b) **What dies the background look like? The structural beam in Figure 1 doesn't have any steel in it? There is no change of the background over time? Or how did you handle the background removal?**

   **Response:**

   i. There isn't any steel in the structural pole because the room was general magnetic measurement, so only non-magnetic material was used.

   ii. The background changed with time because the measurement was conducted on separate days. Therefore, the data shown in the manuscript have been diurnal-corrected and background corrected as it is stated in the caption of the figure.

   iii. The process can be expressed as
   **Corrected magnetic signature** = (**Raw magnetic signature**−**Diurnal variations**)− (**Raw background measurement** − **Diurnal variations**).

(c) **You may want to add what gridding algorithm was used or if a filter was used. If an exact gridding algorithm was used without a filter, great job! iv. Why is there no signature from the motors? Or were they removed? v. What is the signature located in the tail seen in Figure 2b)**

**Response:** Yes, we clarified in the manuscript how we gridded the data in the manuscript. Only a simple linear interpolation that is a built-in function in Matlab was used to grid the data, no extra filtering was involved. There is the signature from the the motors, but the signature from the motors is masked by the magnetic signature from the highly magnetic servomotors. It is much easier to see in Figure 3c.

(d) **P6, line 122. I do not understand why the flexibility of the wing from Tuck et al. 2018 would provide a limit on the flexibility of the wing of this UAV?**

**Response:** We rephrased the sentence.

(e) **Could you use the same colour bar for a) b) and c) in Figure 2.**

**Response:** We tried to use the same color scale. But because the direction of the magnetic field was changed as the orientation of the UAV was changed, so if we use the same color scale for the three figures, the magnetic highs and lows you see in Figure 3 will not be as clear as they are now. For example, the magnitude in Figure 3a is from -200 nT to around +680 nT, whereas the magnitude in Figure 3c is from -730 nT to 160 nT.

(f) **Two reference that would be well suited for this section: 1. (Hansen, 2018) – magnetically modelled a fixed-wing VTOL UAV. 2. (Tuck, 2019) – magnetically characterized 4 different UAVs using a motor setup.**

**Response:** We referenced the two articles as suggested.

## Specific comments

1. **The motors seem to have many names: "electric engines" (P1, line 10), "BLDC motor" (P4, table 1), "BLDC servomotor"(Figure 3 caption). Personally I prefer "BLDC motor" as I think of servo when I read servomotor and pistons (like a gasoline engine) when I read engine. As a result, I am confused whether 3b is the magnetic signature of a servo or the motor. As there are 4 of the former and 3 of the latter how does their signatures compare among each variant? (Forrester, 2011) suggest that the field produced by servos can vary significantly.**

   **Response:** We see the confusion. We use, therefore, servomotor and motor instead. In comparison with the original servomotors that came with the UAV, the new servomotor is 10 times less magnetic.

2. **I could not find a reference to figure 3**

   **Response:** Please see the reference of the figure at Line 103.

3. **Are there tail servos? Where are they in figure 3?**

   **Response:** Yes, there are three servomotors, two for the elevator and one for the rudder. In Figure 4b in the manuscript or the following figure 1, we can see three magnetic highs that should be associated with the back servomotors and the rear motor.

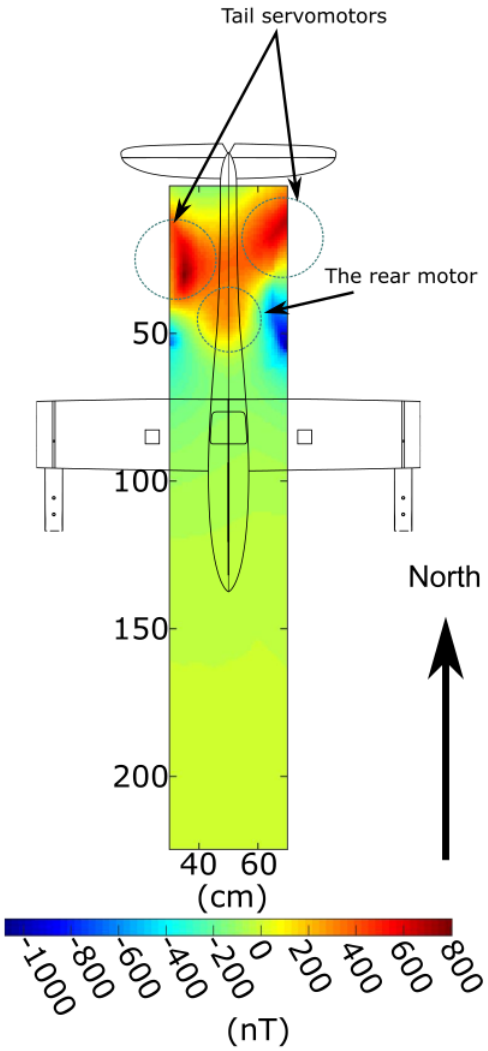


Figure 1: Location of the tail servomotors and the rear motor.

4. **P2. Line 38. Are traditional manned aeromagnetic surveys limited to above 80m? Can you provide a reference for this? I have seen helicopter mag surveys searching for UXO only a few metres off the ground. . .**

   **Response:** In *Aeromagnetic Surveys: Principles, Practices, and Interpretation* by Colin Reeves, on page 44, it states that conventional fixed-wing survey aircraft in terrain free of significant topography are routinely operated at terrain clearances of 100 m, 60 m, and even 30 me in some countries. However, in all EU member states, Visual Flight Rules set out a minimum altitude of 150 m (500 ft). We see the confusion, we rephrased the sentence.

5. **P2, Line 39. I would suggest adding something about the improvement of detectability by 1/distance^3. This is important!**

**Response:** We rephrased the sentence.

6. **P3,line 61. Tuck et al propose a method for characterization that incorporates both static and dynamic interference together by powering the motors during measurement. The "interplay" is relevant to how a source can influence other sources and so all systems should be active during characterization. Could you be clearer as to why you claim this experiment is still not sufficient? Also, you do not do this for your characterization experiment and should be explained why you chose to ignore this "interplay"**

   **Response:** We agree with Tuck that measuring the magnetic signature of each component of a UAV is very helpful to understand the magnetic interference from a UAV. But the magnetic signature of a UAV can become rather complex and dynamic, especially when all electric motors and servomotors and electronic components switch on. As a result, the magnetic signature of a UAV can vary dramatically, which depends on a plethora of factors such as power consumption, throttling, attitude, and even on-site air density as well as air speed. Therefore, we recommend not only to measure the static magnetic signature of a UAV but also to fly the UAV and collect in-flight magnetic data to analyze the real-time in-flight magnetic interference from a UAV.

7. **P3, line 71. Are the motor still powered during fixed-wing flight to keep the props from spinning? Or do they loosely spin during flight? Wouldn't either scenario provide interference?**

   **Response:** The front motors are still powered in the cruise mode (or the fixed-wing mode) but should not rotate (please see the attached figure that shows the status of the two front motors). In principle, as long as a brushless DC motor rotates, there is an alternating magnetic field generated by the spinning rotor that includes a few permanent magnets.


Figure 2: Status of the front motors in the cruise mode. The figure is credited to Kapetair.

8. **P5, line 106 you say "The UAV remained turned-off during the magnetic signature measurement".**

   **Response:** We rephrased the sentence.

9. **Sentence on P5, line 114-116 is not true. The noise envelope is not a function of the efficiency of compensation.**

   **Response:** We agree that the noise envelop is not a function of the efficiency of compensation. We see the confusion, and we deleted the confusing part.

10. **P7, line 137. It should be noted that although increasing the boom length may not create additional significant aerodynamic forces, it does increase instability during flight. Also, one would expect larger amplitude vibrations with a longer boom (P7, line 141).**

    **Response:** Yes we agree. But as our aero-engineer (the second author) has pointed out that it should not increase instability as long as the center of gravity of the UAV stays where it is supposed to be by adjusting the battery's position and the flight controller is able to handle the changes in the moment of inertia. As for the in-flight vibrations, by using a strong rod or a rigid tube with a properly designed supporting structure, the vibrations can be kept to a minimum. Furthermore, the added length of the rod increases the arm of the aerodynamic forces. This does have a negative impact on the stability specially on pitch and yaw states, but the impact is kept within the controllable ranges of the flight controller and aerodynamic control surfaces (elevator and rudder).

11. **P9, line 179. Are you suggesting that the magnetic geology 12 km deep created a gradient of 225nT/m? Later you say otherwise (p10, line 187) so I think you just need to reword this sentence.**

    **Response:** We rephrased the sentence as suggested. The local geology should not create such strong gradient, which must be from the UAV.

12. **P10, line 180. You suggest the interference is "probably due to radio transmission and cultural noise". You could test this by turning your radio on and off. You can test for cultural noise by moving the UAV to another area.**

    **Response:** We agree with the reviewer that we could have done that. Because we are also new the development of a UAV-borne system, we didn't expect that the cultural noise in the vicinity of the test site and the radio transmission could be measured by the magnetometers.

13. **Figure 8. Why doesn't the 4th difference correlate between the two sensors if the source is mainly the UAV? Perhaps worthy of discussion?**

    **Response:** Because the attenuation due to distance is strong, that is why in the figure the the secondary magnetic profile is a lot noisier and the 4th difference of the primary magnetic profile is almost constant, which means that some of the interference that can be measured by the secondary sensor may be too small to be measured by the primary sensor. Therefore, the 4th difference of the two magnetic profiles may not necessarily be correlated.

14. **P13, line 2. Will adding 10 cm to L make much of a difference? This can be calculated easily once you identify your source (which you do in the previous section).**

**Response:** Yes, the data that we show in the manuscript are the raw observations. We were surprised by the big difference due to the 10 cm difference as well. Since the major noise source is the output current, it is dependent on the magnitude of the output current from the battery, the shape of the current-carrying cable, and the orientation of the current-carrying cable, which make it difficult to calculate the resultant magnetic field.

15. **P13, line 231. Either use relative time or do the math. Relative time looks cleaner**

    **Response:** We re-plot the figures using relative timestamp as suggested.

16. **P17, line 251. Why is the gradient higher for the second dynamic experiment than the first?**

    **Response:** There are several reasons as we stated in the manuscript. First of all, the there were GNSS antenna and IMU in the cockpit in the first dynamic experiment. For the secondary experiment, the GNSS and IMU were removed after the timestamp was synchronised. Besides, due to the weight change, we had to re-adjust the location of the battery to make sure the CG stays where it should be so that the layout in the cockpit was changed and meanwhile the shape of the current-carrying cable and orientation of the current-carrying cable were alos changed. The main reason should be the changes made to the current-carrying cable.

# Reviewer #2

## General Comments

1. **Does the abstract provide a concise and complete summary? Asses the possibility to shorten the Abstract.**

   **Response:** We shortened the abstract to make it concise and readable as suggested.

2. **Few figures and tables outside their respective areas. PG 5 line 103 I would move the Figure 1 after the line 106, FIG 15 out of place. Make sure the final document have figures in proper places.**

   **Response:** We changed the layout as suggested.

3. **I did run a grammar software and found 45 items, few plural words were missing, but overall a good grammar check where done, Few items such as Line 92 UAV's "own" magnetic, Line 200 "Apparently", Line 210 "owing to the fact that", Line 235 "It is evident that", Line 266 wires can "actually", Could be replaced or even removed. My system did recognized few non American variations of the words.**

   **Response:** We revised the texts as suggested.

4. **I would recommend to add an aircraft blueprint to include locations of items such as servos like found in Figure 3, But improve it the missing the PG 2 line 47 & 73 global positioning system (GPS) Replace to GNSS the non commercial name.**

   **Response:** We provided an aircraft blueprint to include locations of items as suggested.

5. **In the specifications, the stall speed is with Nose "cone", if is without, state the configuration, did any performance in stall speed was found, even by changing the items inside? Specially range of operation, it has changed? an important item for companies. And or changing the angle of the nose rod for magnetometer better position in level flight.**

   **Response:**

   (a) The stall speed should not change with the boom because the boom does not change the aerodynamic properties of the wings.

   (b) The range of operation should be slightly reduced because of the drag introduced by the boom and the additional weight of the payload.

   (c) As shown in Table 2, the dead zone of the magnetometer is the equatorial plane $\pm$ 7 degrees, so the magnetometers have to be tilted properly according to the direction of the local geomagnetic field to have good measurements.

6. **Fig 2, Is possible that the motors are Counter-rotating, thus having on each wing a higher Nt closest to the tip, but also might be redundant since in cruse flight those motors are off, and producing if any a small portion of electricity.**

   **Response:** As long as a motor spins, there will be electricity. It will work like a small generator.

7. **Line 123 is mentioned the wing flex, by the elliptical wing shape it might need a modification to support it but some aircraft have an extension on wingtips by a boom, It does increase drag especially during climb, but data is received within parameters. Also mentioned that the carbon fiber line 85, is considered to install static wicks on the surfaces to compensate for it?**

   **Response:** We are developing an active compensation algorithm to reduce the magnetic interference due to the eddy current in the wing. But in principle, the area the of the wing is fairly small, only up to 1 $m^2$, so the magnetic interference due to the eddy current should be fairly small as well.

8. **One of many issues I have in survey is the wire connection and wire loose in the fuselage (as mentioned) specially near connectors.**

   **Response:** We agree with the reviewer. Therefore, we will try to put the current-carrying cables in the back of the fuselage. If necessary, we may try to use some special material to shield the magnetic field generated by the current.

# Experiments on magnetic interference for a portable airborne magnetometry system using a hybrid unmanned aerial vehicle (UAV)

Jirigalatu Jirigalatu, Vamsi Krishna, Eduardo Lima Simões da Silva, and Arne Døssing

CMAGTRES, Technical University of Denmark
Centrifugevej Bygning 356
2800 Kgs. Lyngby, Denmark

**Correspondence:** Arne Døssing (ards@space.dtu.dk)

**Abstract.** ~~Airborne magnetic surveys are an important and efficient tool for mapping the subsurface, providing insights e.g. into mineral deposits. Compared to traditional ground methods, airborne magnetic surveys offer great advantages with~~ Using UAVs for airborne magnetometry offers not only improved access and rapid sampling ~~. But the cost and hassle of transporting and operating a conventional manned airborne magnetic survey system are strong impediments for its wider use. In addition, the conventional airborne systems are challenged by the need for low-altitude (≤80 m) surveying to detect small-scale subsurface features~~ but also reduced logistics costs. More importantly, the UAV-borne aeromagnetometry can be performed at low altitudes, which makes it possible to resolve fine features otherwise only evident in ground surveys. ~~Portable and compact airborne magnetic survey systems using unmanned aerial vehicles (UAVs) can not only bridge the gap between conventional airborne magnetic surveys and ground magnetic surveys but also complement magnetic surveys to fit broader geophysical applications. Therefore, developing high-quality, stable, and portable~~ Developing such a UAV-borne ~~survey systems is of high interest to the geophysical exploration community. However, developing such a~~ aeromagnetometry system is challenging owing to strong magnetic interference introduced by onboard electric ~~engines and other onboard electronic devices. As a result, tests~~ and electronic components. An experiment concerning the static ~~and dynamic~~ magnetic interference of ~~a UAV are critical~~ the UAV was conducted to assess the severity of the interference ~~and can help to improve the design of the system at the early stage of development. A static experiment and two dynamic experiments were conducted to understand the characterization of the magnetic interference of our~~ of a hybrid vertical take-off and landing (VTOL) UAV. The results of the static experiment show that the wing area is highly magnetic due to the proximity to servomotors and motors, ~~but~~ whereas the area along the longitudinal axis of the UAV ~~is relatively magnetically quiet. To reduce the magnetic signature, the highly-magnetic servomotors on the wings were replaced with less magnetic servomotors of a brush-less type~~has a relatively smaller magnetic signature. Assisted by the static experiment and aerodynamic simulations, we ~~further designed~~ first proposed a front-mounting solution ~~for~~ with two compact magnetometers. ~~Two~~ Subsequently, two dynamic experiments were conducted with ~~this setup to understand~~ the setup to assess the dynamic interference of the ~~UAV in operation~~system. The results of the dynamic experiments reveal that the strongest source of in-flight magnetic interference is ~~mainly due to the~~ the current-carrying cables connecting the battery to the flight controller and that this effect is most influential during pitch maneuvers of the aircraft.

## 1 Introduction

Magnetic surveying has been extensively used in the search for mineral deposits, oil and gas reservoirs, geothermal resources, as well as for a variety of other purposes such as natural hazards assessment, basement structural studies, mapping subsurface archaeology, and unexploded ordnance (UXO) ~~(Nabighian et al., 2005; Eppelbaum, 2011; Fairhead, 2012; Hinze et al., 2013; Eppelbaum, 20~~ (Nabighian et al., 2005; Hinze et al., 2013; Kruse, 2013; Haldar, 2018; Turner et al., 2015). In general, magnetic measurements can ~~provide information on and~~ give insight into the physical, chemical, and even biological processes that have affected the iron phases within.

Airborne magnetometry (aeromagnetometry) is an inexpensive, efficient, and effective regional reconnaissance tool ~~(Reeves, 2005; Eppel~~ (Reeves, 2005). The method offers improved accessibility to areas restricted to terrestrial surveys such as remote areas, offshore areas, and thickly-vegetated regions as well as a rapid sampling of the local geomagnetic field compared to its ground or space counterpart (Council, 1995; Haldar, 2018).

~~Traditionally~~Conventionally, aeromagnetic surveys are often conducted using ~~fixed-winged~~ fixed-wing aircraft with sensors mounted on both ~~the~~ wings (horizontal sensor configuration) or a ~~tail-boom~~ tail-stinger behind the aircraft. Thanks to decades of development ~~and~~ in noise reduction techniques coupled with new advances in sensor technologies, such modern aeromagnetic surveys can achieve a sensitivity of 0.1 nanoTesla (nT) ~~(Eppelbaum, 2015; Aminzadeh and Dasgupta, 2013; Turner et al., 2015) . However, geophysicists~~ (Eppelbaum, 2015; Turner et al., 2015). Geophysicists have realized that aeromagnetometry using light-weight and compact platforms such as unmanned aerial vehicles (UAV) can even further reduce ~~the surveying cost and make it more convenient in terms of logistics~~ surveying costs (Eppelbaum and Mishne, 2011; Tuck et al., 2018; Mu et al., 2020). ~~Besides, traditional manned aeromagnetic surveys normally operate at 80 meters or above for the safety of personnel and because of flight regulations, whereas~~ More importantly, UAV-borne magnetometry systems are capable of flying ~~at a lower altitude~~with low terrain clearances, thereby improving detectability ~~(Reid, 1980; Reeves et al., 1997; Eppelbaum and Mishne, 2011; Zhou,~~ significantly (Eppelbaum and Mishne, 2011).

In the recent decade, the feasibility and effectiveness of light-weight UAV-borne magnetometry systems have been demonstrated ~~again and again~~ by various geophysical applications, from identifying various rock types and structures in the subsurface and delineating ore deposits to locating man-made ferrous objects, such as UXO (Perry et al., 2002; Cunningham, 2016; Malehmir et al., 2017; Parvar et al., 2017; Kolster and Døssing, 2020). However, developing a low-noise ~~and efficient~~ UAV-borne magnetometry system is challenging given the compact ~~space~~ size of a UAV platform, i.e., magnetometers ~~readily~~ easily fall in the vicinity of sources of magnetic interference from the platform, such as motors, ~~electric powered~~ electric-powered devices, and even current-carrying ~~wires (Forrester, 2011; Sterligov and Cherkasov, 2016; Tuck et al., 2018)~~cables (Forrester, 2011; Sterligov . As a result, UAV-borne magnetometry systems are ~~operated often by suspending a so-called~~ often suspended in a magnetometer bird (housing magnetometers, global ~~positioning system (GPS~~navigation satellite system (GNSS) antenna and data logger) a few meters below the airframe to minimize the interference from the platform (Malehmir et al., 2017; Parvar et al., 2017; Parshin et al., 2018; Sterligov et al., 2018; Nikulin and de Smet, 2019). This configuration is hardly prone to the ~~onboard~~ magnetic interference from the platform but ~~comes with a~~ at the cost of efficiency and positioning accuracy (Tuck et al., 2018).

Alternatively, magnetometers may be mounted directly on a boom attached to the UAV airframe (Samson et al., 2010) or on the wing-tips of the platform (Wood et al., 2016).

To facilitate ~~high-quality~~ high-resolution and efficient UAV-borne magnetometry, we ~~intend~~ intended to develop a lightweight (less than 10 kg), efficient (more than 70 km per charge), and flexible (vertical take-off and landing) UAV-borne magnetometry system, capable of conducting magnetic surveys in various terrains. To meet the requirements, we chose a hybrid ~~lightweight~~ fixed-wing UAV platform capable of taking off and landing vertically. ~~But where and how to put the magnetometers on the UAV are the first challenge we have to face. Hence~~To determine the optimal placement of the magnetometers, a good understanding of the magnetic interference of the platform is necessary at the early stage of the development. For example, Forrester (2011) and Sterligov and Cherkasov (2016) successfully mapped magnetic signatures of the UAVs and also managed to locate sources of interference. However, they neglected to address the complex interplay between active and passive components (Tuck et al., 2018). Therefore, Tuck et al. (2018) proposed a systematic method to investigate magnetic interference of UAVs and demonstrated their method on a 25 kg fixed-wing UAV. ~~However, the method is still not sufficient to cover the actual interplay between static interference and dynamic interference in operation. In this paper~~Instead of investigating every possible source from the platform, we will present a static and two dynamic experiments to investigate both the static and dynamic magnetic interference as well as their interplay from the platform in operation.

## 2 Platform - A hybrid VTOL UAV

The UAV for ~~our~~ the airborne magnetometry system is a beta prototype version of a hybrid vertical take-off and landing (VTOL) UAV from Kapetair. ~~As the name of the UAV indicates, the UAV~~ The UAV is capable of taking off and landing vertically without a runway, so it can be deployed in various terrains. ~~Since the UAV is a hybrid,~~ And it is capable of flying ~~both in~~ in both multi-rotor mode and fixed-wing mode. The UAV has three position-adjustable motors. The two front motors are ~~mainly used for taking off and landing~~used for multi-rotor mode. The third (tail) motor is used for take-off and landing as well as to provide thrust during the fixed-wing/cruise mode, i. e., the front ~~motor stays~~ motors stay inactive during the cruise mode and only the rear ~~engine~~ motor remains active. The ~~main~~ fuselage of the UAV houses various hardware components, including a flight controller (FC), several electronic speed controllers (ESC), an inertial measurement unit (IMU), a global ~~positioning system (GPS~~navigation satellite system (GNSS) module, a radio-frequency (RF) module, a data-logger for magnetometry, and a few ~~wires or~~ cables connecting those components. A 22000 mAh Li-Po battery is also placed ~~inside in the~~ in the front of the fuselage. The technical specifications of the platform are listed in Table 1.

### 2.1 Source of magnetic interference

For a lightweight UAV platform such as the Kapetair VTOL UAV, brushless direct current (BLDC) motors are often used due to their better speed control, higher efficiency, and compact design ~~A. D. P. Juliani et al. (2008). However,~~ (A. D. P. Juliani et al., 2008) . BLDC motors comprise permanent magnets and solenoids~~. Hence, the electric engines and the servomotors~~ , which can generate a strong magnetic signature~~even when they are off and leakage of a strong magnetic field when they are on. Besides, the~~ . The

**Table 1.** Specifications of Kapetair VTOL UAV

| Component of the UAV | |
|---|---|
| Dimensions (wingspan×length) | 3300 ×1670 mm |
| Batteries | 1 × 6S Li-Po 22.2V 488.4 Wh 22000 mAh |
| Servomotors on the wings | 4 × HBL 6625MINI Metal Alloy Gear |
| Propulsion system | 3 × T-Motor MN5212 KV420 BLDC motor |
| Flight controller | ~~Pixhawk 2~~ 1 × Pixhawk 2.1 cube black |
| ~~Payload weight 1000 g~~ Cruise speed | 65 km/h |
| Aircraft gross weight | 6.5 kg |
| Payload weight | 1000 g |
| Stall speed (airplane mode) | 20 km/h |

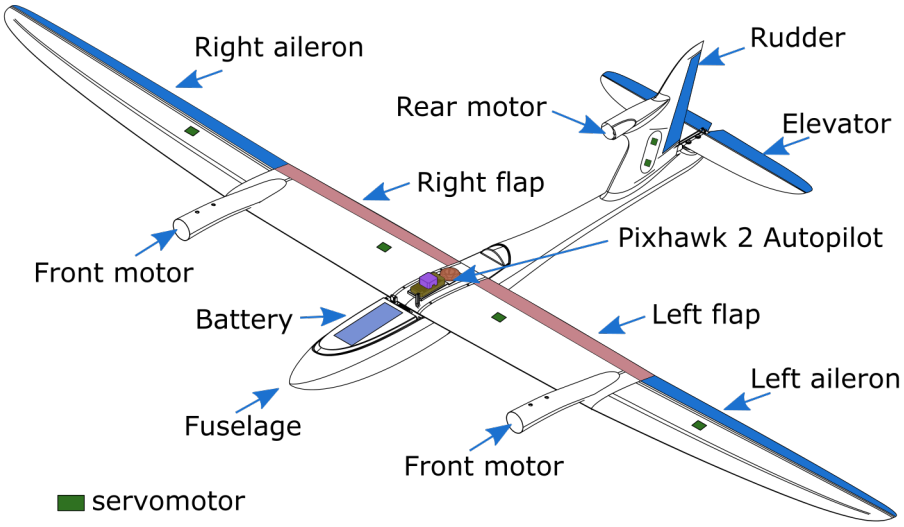


**Figure 1.** Schematic view of the layout of the UAV.

BLDC motors are driven to revolve ~~at the desired speed by sending properly~~ by sending tuned pulses of current to the solenoids, which means constant electrical switching, probably causing discontinuous ~~in-flight magnetic measurements~~magnetic interference. Tuck et al. (2018) observed magnetic interference due to the current-carrying ~~wires~~ cables connecting the ESC to the batteries. According to Ampere's law, the magnetic field is proportional to the electric current~~, therefore,~~. Therefore, the magnetic interference varies with the current in the ~~wires. Moreover~~cables. Also, the airframe of the UAV is composed of carbon fiber, which is non-magnetic but conductive, akin to graphite (Chung, 2010). As a result, eddy currents (Richard L., 1974) may play a role in magnetic interference during ~~a~~ flight. Finally, the onboard avionics system which comprises several electronic components (such as the FC module, the IMU module, the ~~GPS~~ GNSS module, etc.) may generate complex electromagnetic interference.

A rule of thumb is~~therefore~~ , therefore, always to place magnetometers as far away from the ~~magnetic UAV components~~ UAV components that are magnetic as possible.

## 3 UAV magnetic signature mapping - static experiment

An airborne magnetometry system using a compact UAV platform is affected by the UAV's magnetic signature (Tuck et al., 2018). Mapping the magnetic signature of a UAV is useful to identify magnetic highs and lows of the UAV ~~'s own magnetic field and helps us to avoid magnetic highs when developing our magnetometry system and pinpoint the~~ and pinpoint favorable regions less susceptible to the UAV's magnetic interference. ~~However,~~ Because the magnetic signature varies from platform to platform, ~~and it is therefore~~ it is imperative to map a specific platform's ~~specific magnetic signatureto identify sources of interference and pinpoint optimal regions on the aircraft for mounting magnetometers.~~ magnetic signature.

### 3.1 Method

The magnetic signature mapping of the Kapetair UAV was carried out at the Brorfelde geomagnetic observatory in Denmark. A customized 2300×958×700 mm wooden frame was built for the experiment (Fig 2). Since the magnetic signature of a UAV can change significantly over a few centimeters, it is beneficial to have the magnetic signature on a fine grid with cells of such as a 10×10 cm ~~cell~~ (Sterligov and Cherkasov, 2016). However, such an approach is time-consuming if carried out manually. We adopted a slowly revolving DC motor to pull a slider holding a high-precision potassium scalar magnetometer (GSMP-35U from GEM Systems). The sampling rate of the magnetometer was set to 10 Hz and the speed of the slider was 2 cm/s on average. The DC motor, a laptop for data logging, and two power supplies were placed in another room away from the measurement. Due to the limited space in the observatory, only one wing and the mainframe were measured at once (Fig 2). The UAV remained ~~turned-off~~ off during the magnetic signature measurement.

### 3.2 Magnetic signature

With the help of the semi-automatic magnetic measurement, we ~~managed to collect~~ collected more than 70000 magnetic observations of the ~~UAV magnetic signature, including~~ magnetic signatures of the starboard wing, the port wing, and the area along the longitudinal axis of the UAV~~(Fig 3)~~, together with their respective background field. The background fields and the magnetic signatures experienced diurnal corrections. After the diurnal corrections and background removal, the corrected magnetic signatures were gridded on a planar surface with a 2.5 cm grid interval shown in Fig 3. As seen in Fig 3 the magnetic signature of the wing area has a high amplitude (up to ~~+~~600 nT) and peaks over the servomotors and the motors. ~~Interestingly, the servomotors signal is asymmetric, being significantly higher over the outer starboard wing as compared to the outer port wing. As expected the servomotors signal rapidly decreases~~ The servomotors make a major contribution to the overall magnetic signature of the UAV, their magnetic signatures decrease rapidly with distance, also towards the main fuselage of the platform. ~~It is axiomatic that the servomotors make a major contribution to the magnetic signature. However, for a~~ For a high-resolution aeromagnetic system, the standard of commercial aeromagnetic practice that only allows a noise envelope of 0.1 nT ~~after~~

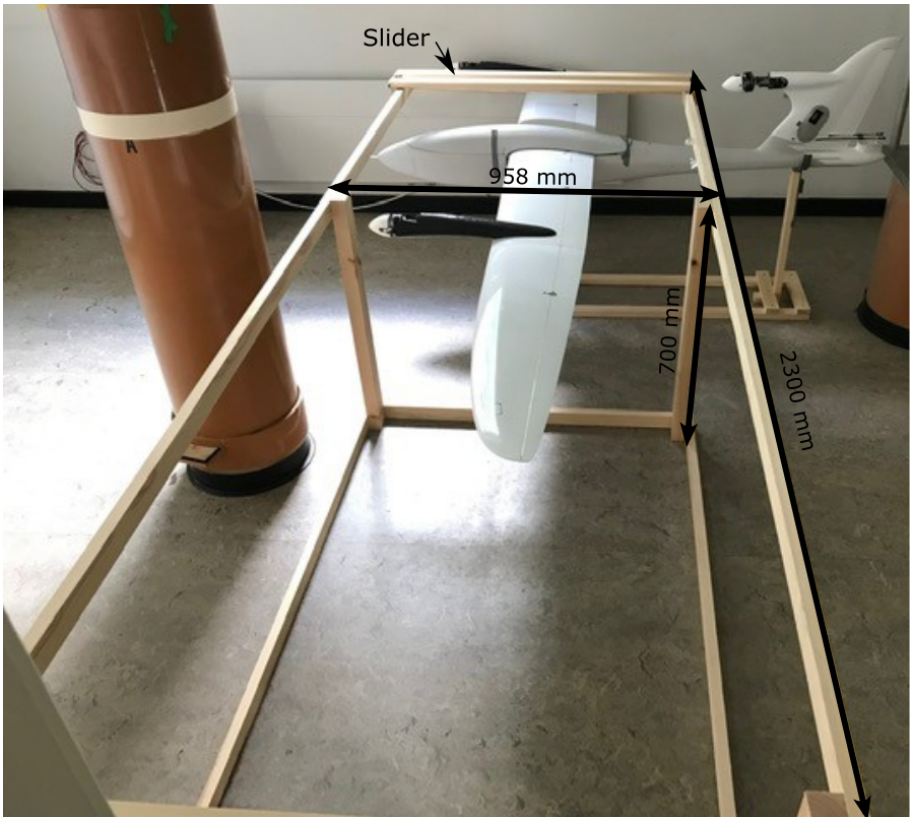


**Figure 2.** Demonstration of the magnetic signature measurement of the port wing. The length and the width of the slider are 1000 and 150 mm, respectively.

~~compensation, assuming that post compensation can remove 95% percent or more of interference from aeromagnetic data Reeves (2005); Tuck et al. (2018). This, on the other hand,~~ (Reeves, 2005) requires the magnetometers to be mounted in places with the least magnetic signature. Due to the high magnetic ~~signature~~ signatures of the servomotors, we ~~decided to replace~~ replaced the originally highly magnetic servomotors with ~~more expensive~~ BLDC servomotors with a smaller magnetic signature (see ~~4~~Fig 4b).

According to the map of the magnetic signature (Fig 3), the wing-tips and the nose-tip are magnetically low-amplitude zones. Mounting two magnetic sensors at the tip of the wings ~~enable us~~ renders it possible to measure the horizontal gradient, which is useful for both data processing and interpretation purposes. However, the wings are deliberately flexible to adapt to dynamic airflow in flight, i. e. the high-frequency vertical displacement due to the flexibility (readily up to 120 mm~~during flight (Tuck et al., 2018))~~ ) during flight may introduce unpredictable noise ~~Kaneko et al. (2011)~~(Tuck et al., 2018). Moreover, aerodynamically, the wingtips are sensitive to the disturbance caused by geometric changes, i. e., mounting magnetometers onto the wings' exterior may lead to wing stall and even a crash.

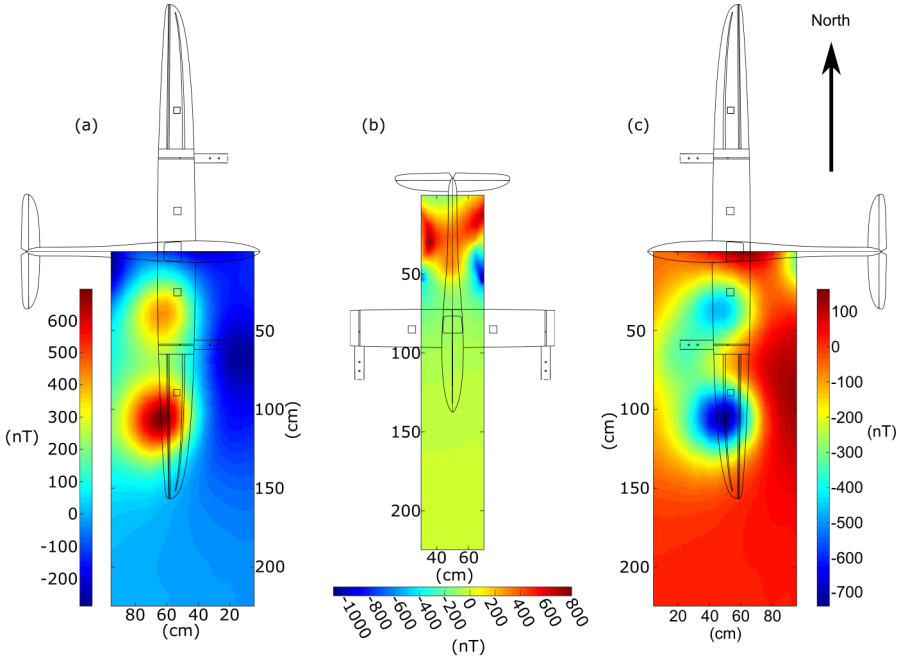


**Figure 3.** The diurnal-corrected and background-subtracted magnetic signature: (a) the starboard wing, (b) the area along the longitudinal axis of the UAV, and (c) the port wing.

## 4 A front-boom setup

Mounting magnetometers on the nose-tip does not provide ~~a~~ the typical horizontal gradient but ~~, on the other hand,~~ provides an aerodynamically ~~safe and stable solution . To avoid the risk of aerodynamic instability, we designed a magnetometry system mounting on the nose of the UAV using protruding carbon rods~~ stable solution (see Fig 5). This configuration will theoretically not cause any aerodynamic instability because the geometric modification to the nose area should cause only small aerodynamic forces. We carried out a computational fluid dynamics (CFD) simulation on the fuselage to investigate the aerodynamic stability of the nose setup. The plot (Fig 5: lower panel) shows that the influence introduced by adding the mount on the nose is negligibly small with the maximum magnitude of lift forces being around 1 N (compared to the total lift force of the UAV ~~, up to~~ during leveled flight, of around 60 N ~~(~~as it should balance a mass of 6 ~~Kg~~kg). In principle, the center of gravity (CG) can be fixed by adjusting the battery position and some changes in the moment of inertia can be easily handled by the flight controller. A flight test with this setup showed stable behavior of the UAV, ~~and~~ confirming that the change in the moment of inertia is within the capabilities of the flight controller. ~~Increased boom lengths theoretically do~~ And increasing the boom length does not cause significant aerodynamic forces as long as the rod is ~~parallel to the airflow or~~ kept at small angles ~~of attack during the~~ with the airflow during flight.

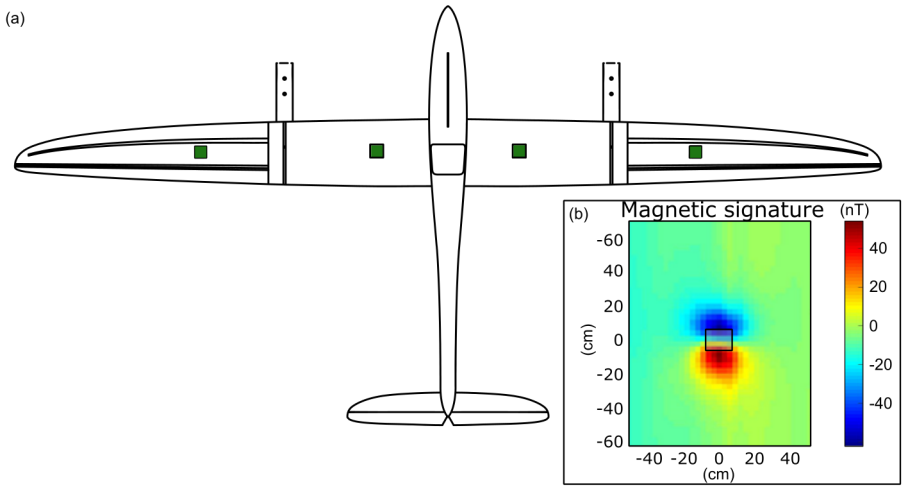


**Figure 4.** Locations of the replaced servomotors and the magnetic signature of the new BLDC servomotor: (a) the locations of the replaced servomotors, ~~which are~~ indicated by green squares, (b) the magnetic signature of the new low-magnetic servomotor, and the small black square in the middle indicates where the servomotor was located and the servomotor was ~~powered~~ off during the measurement. The measurement was conducted on a planar 10 cm above the ~~servo~~servomotor.

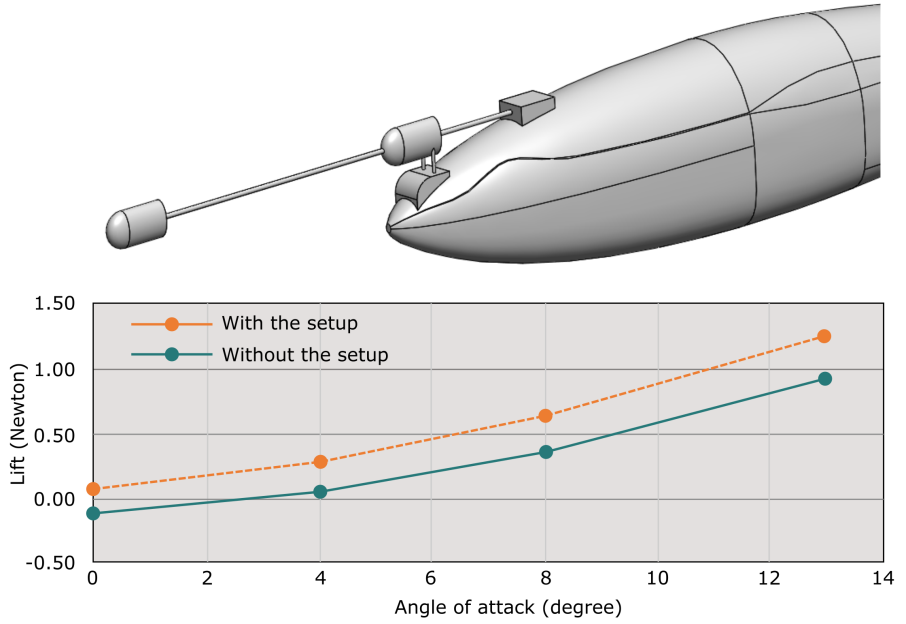


**Figure 5.** The nose-mounting solution and its ~~aerodynamics simulation~~aerodynamic forces.

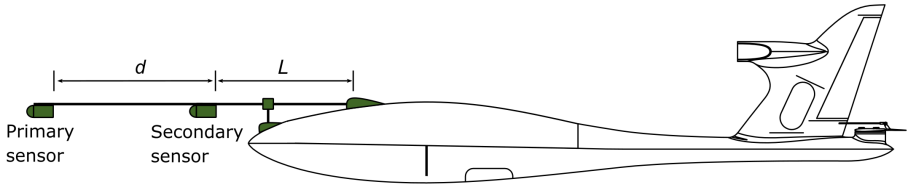


**Figure 6.** ~~The final design~~ Side view of the final front-boom-mounting setup~~and a side view of the hybrid VTOL fixed-wing in this study~~.

**Table 2.** Specifications of QuSpin Total Field Magnetometers (QTFM)

| Parameters | |
|---|---|
| Field sensitivity | smaller than 1pT in 0.1 Hz - 100 Hz band |
| Dynamic range | 1000 nT to 100000 nT |
| Max data rate | 400 samples/s |
| Dead zone | single equatorial plane, $\pm$7 deg |
| Atomic species | Rubidium |
| Power | 5V to 19V, 2 W total (sensor+electronics), 3W during startup |
| Heading error | below 3 nT (uncompensated) |

Based on the ~~result~~ results of the static experiment and the aerodynamic analysis, ~~we slightly tweaked the initial set-up as shown in Fig 5, still mounting~~ some changes were made to the initial setup (Fig 5), resulting in the two magnetometers on ~~a boom mounted on the noise-tip but now with both sensors~~ the boom now being placed further away from the aircraft (Fig 6) to ~~reduce the amount of noise on the sensors and provide a solution where filtering out~~ further reduce the magnetic noise from the UAV~~becomes easier (Chen et al., 2018; Mu et al., 2020).~~

~~The second iteration of the setup comprises the installation of~~ . Meanwhile, the two-magnetometer setup provides a solution that eases the filtering of the magnetic noise (Chen et al., 2018; Mu et al., 2020). The two compact magnetometers ~~from~~ are manufactured by QuSpin, abbreviated as QTFM. The QTFM is a compact, low power, and high-sensitivity scalar magnetometer, capable of sampling the geomagnetic field over 200 times per second (Table 2). The primary magnetometer (front magnetometer) is responsible for ~~measuring the signal of interest~~observing the geomagnetic field, whereas the secondary sensor placed closer to the nose-tip is used to monitor the in-flight noise from the platform. The distance $d$ is used to indicate the distance between the primary and secondary magnetometer, whereas $L$ is for the distance between the secondary magnetometer and the mounting point on the UAV (see Fig 6).

## 5 UAV in-flight magnetic signature - dynamic experiment

To understand the real dynamic noise of the UAV in operation, we flew two dynamic experiments in Støvring, Denmark (Fig 7). The test site is covered with up to 12 km of unmetamorphosed sediments lodged over the crystalline basement, and the surface of the region consists mainly of unconsolidated Quaternary glacial and interglacial deposits (Håkansson and Surlyk, 1997). Normally, sediments are considered non-magnetic, which is the basis for many applications of aeromagnetic surveys (Reeves, 2005) . As a result, the local magnetic field is insignificant, which renders the data collected during the dynamic experiment a direct reflection of the dynamic noise from the platform.

### 5.1 Method

Dynamic effects ~~such as magnetic field generated by revolving solenoidsor~~ that originate from revolving solenoids, permanent magnets, eddy ~~current in the airframe, or maybe even loose wires can produce either discontinuous or~~ currents, or loose current-carrying cables can be divided into discontinuous and continuous noise. ~~Discontinuous~~ The discontinuous noise appears as isolated spikes or set of closely-spaced spikes on ~~the aeromagnetic data~~an aeromagnetic profile, which is typically associated with the pilot's actions such as radio transmissions ~~or~~ and switching direct current~~and to~~ , along with lightning strikes or cultural sources (e.g. train, power lines) (Reeves, 2005; Eppelbaum, 2011, 2015). ~~Continuous~~ The continuous noise comes from the motions of the aircraft, such as the oscillation of wings ~~while in flight through turbulent weather, which produces a high-frequency unwanted noise signal~~due to turbulent weather. The empirical ~~fourth difference function~~ real-time fourth difference is widely used for monitoring the ~~level of such~~ in-flight ~~noise in aeromagnetic data to ensure that the noise is within an acceptable level~~ discontinuous noise in aeromagnetometry (Reeves, 2005). Complying with the widely-accepted industry standard, the fourth difference should lie between $\pm 0.05$ nT (or 0.1 nT peak to peak) (Coyle et al., 2014; Cunningham, 2016). The fourth difference for an airborne magnetic survey can be calculated as

$$\textbf{4th difference} = -\frac{T_{-2} - 4T_{-1} + 6T_0 - 4T_{+1} + T_{+2}}{16}, \tag{1}$$

where $T_{-2}$, $T_{-1}$, $T_{+1}$, and $T_{+2}$ are five consecutive readings centered on the current reading $T_0$.

~~To understand the real dynamic noise of the UAV in operation, we flew two dynamic experiments in Støvring, Denmark (Fig 7). The test site is covered with up to 12 km of unmetamorphosed sediments lodged over the crystalline basement, and the surface of the region consists mainly of unconsolidated Quaternary glacial and interglacial deposits (Håkansson and Surlyk, 1997) . Normally, sediments are considered non-magnetic, which is the basis for many applications of aeromagnetic surveys (Reeves, 2005) . As a result, the local magnetic field is insignificant, which renders the data collected during the dynamic experiment a direct reflection of the dynamic noise from the platform.~~

### 5.2 The first dynamic experiment - multi-rotor mode

The first dynamic experiment was flown on 2020.01.13. The front-mounting boom (Fig 6) was configured as $d$ = 20 cm and $L$ = 20 cm. The sampling rate of the QTFMs was set to 200 Hz. The UAV was switched on ~~and~~ with all required components in position (such as the magnetometers~~and~~ , the power supply for the system, etc.~~, were in position~~). At first, the UAV was placed on the ground ~~and~~ while the pilot was conducting the last-minute check. ~~This led to a moment at which~~ During this

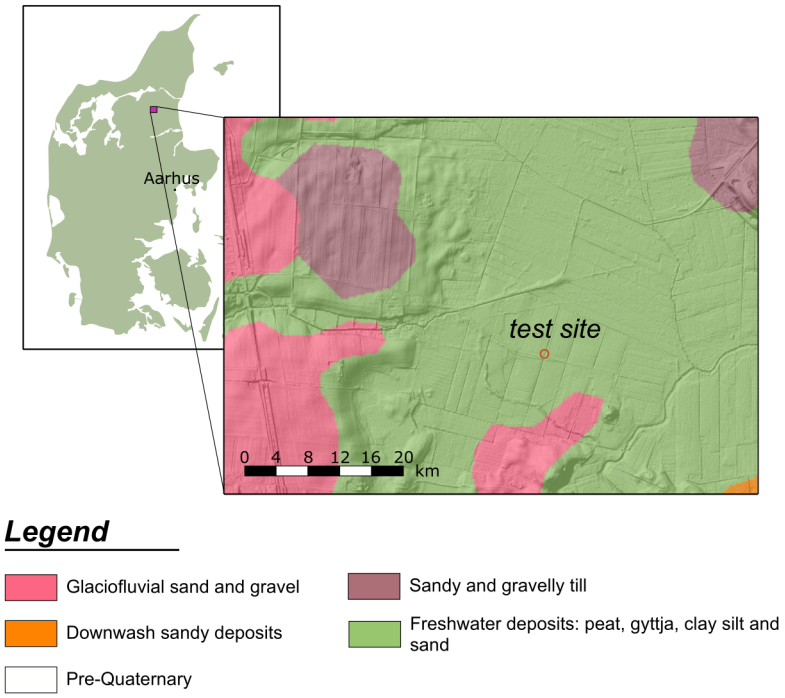


**Figure 7.** Location and surface geology of the test site according to Surface Geology Map of Denmark 1:200000. The surface geology map of Denmark 1:20000 is credited to Schack Pedersen et.al., Surface Geology Map of Denmark, PDF, Version 2, compiled for the scale 1:200000, published in GEUS report 2011/19 (in Danish) by Geological Survey of Denmark and Greenland (GEUS), and the map of Denmark is credited to MAPSVG.COM.

time, the magnetometers could observe dynamic interference from the UAV irrelevant to motions. In this ~~immediate~~ pre-take-off phase (hereafter called "standby phase") and with only a few UAV components being active, the power consumption of the UAV should be low, and the current in the ~~wires~~ cables connecting the battery with the flight controller should be low as well. As a result, the observed magnetic interference in the standby phase should mainly arise from the current-carrying ~~wires in the~~ cables in the front of the fuselage, permanent magnets of the actuators, and radio transmission along with ~~may~~ dynamic and/or static cultural noise in the vicinity. Figure 8 shows residual magnetic intensity (RMI) with the International Geomagnetic Reference Field (IGRF) being removed from the raw magnetic measurements collected in the standby phase. As seen in Fig 8, the plots show continuous ~~measurements of a superimposed magnetic field by the local geology (a constant offset),~~ superimposed effects of the magnetic interference from the UAV, ~~and~~ cultural noise in the vicinity, and the magnetic field by the local geology (probably a constant offset). The RMI ~~in~~ shown in the top panel in Fig 8 is oscillating around 2.8 nT with mean variations less than 0.5 nT, probably due to radio transmission and cultural noise. The average difference between the data from the primary and secondary magnetometer in this configuration is around 45 nT, ~~which means that the longitudinal gradient between the primary and the secondary magnetometers is up to 225 nT/m (45 nT divided by 0.2 m),~~ even when the

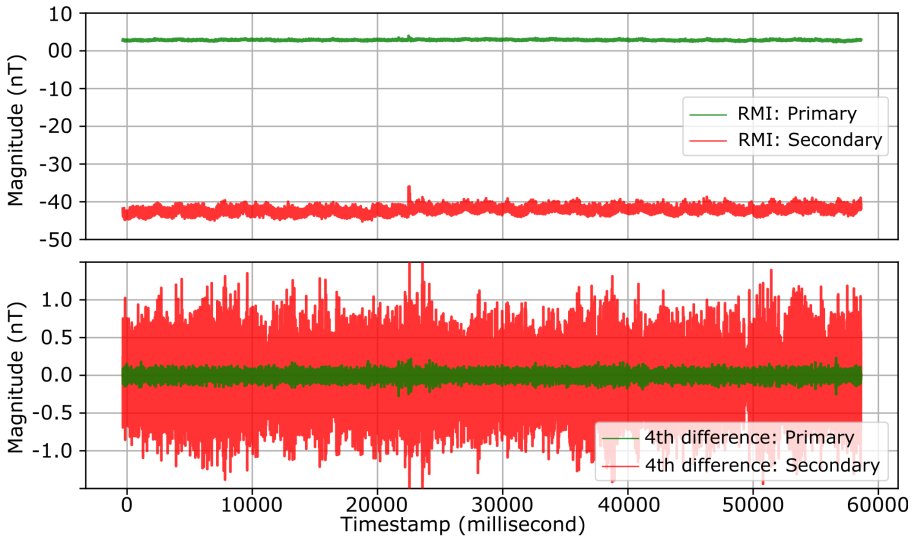


**Figure 8.** Data excerpt of ~~the~~ RMI ~~and the fourth difference~~ profiles recorded by the primary and secondary magnetometer and their respective fourth difference while the UAV was on standby on 2020.01.13 with d = 20 cm and L =20 cm. The IGRF (50560 nT) has been removed.

UAV is on standby. The fourth difference of the measurements from the primary magnetometer is spiky and lies within ±0.15 nT, significantly higher than the industry standard~~. Moreover, the discontinuous noise of the~~ , whereas the fourth difference of the magnetic profile recorded by the secondary magnetometer (Fig 8) is ~~stronger~~even bigger, up to ±1 nT. The difference in the fourth difference indicates that the interference mainly originated from the UAV rather than the surroundings ~~. Otherwise, the fourth difference of the two data sets should be comparable,~~ because the secondary magnetometer is closer to the source of interference~~than the primary magnetometer~~. The distance between the two magnetometers attenuates the interference, leading to the relatively smaller fourth difference of the data outputted by the primary magnetometer.

Following the standby phase, the UAV took off and was flown ~~only~~ manually in the multi-rotor mode~~manually~~. Figure 9 and 10 show the in-flight ~~residual magnetic intensity collected by both~~ RMI collected by the primary and secondary magnetometer ~~together with their corresponding fourth differenceand its flight track~~and their respective fourth difference, together with its flight path. The two ~~plots of the residual magnetic intensity in the figure show an identical pattern. The only~~ RMI profiles in Fig 9 are almost identical in shape. The major difference lies in the magnitude~~with the~~ . The RMI from the primary magnetometer ~~being~~ is 10 times smaller than that from the secondary magnetometer. ~~This~~ The in-flight fourth difference of the primary magnetic profile in Fig 9 is spiky with magnitudes up to ±1 nT, 20 times higher than the industry standard. The increase in the fourth difference is directly associated with the platform. It indicates that the observed signals from the two magnetic sensors ~~were~~ are dominated by the noise from the platform~~itself. An obvious reason for this behavior could be the multi-rotor flight mode with~~ . It could be high output current flowing in the ~~wires~~ cables connecting the flight controller to the battery and the leakage of the alternating magnetic field from the BLDC motors ~~. In the standby phase, we observe a magnetic field of only around 2.8 nT (taken from the primary magnetometer). However, the in-flight fourth difference of the primary data in Fig 9 is~~

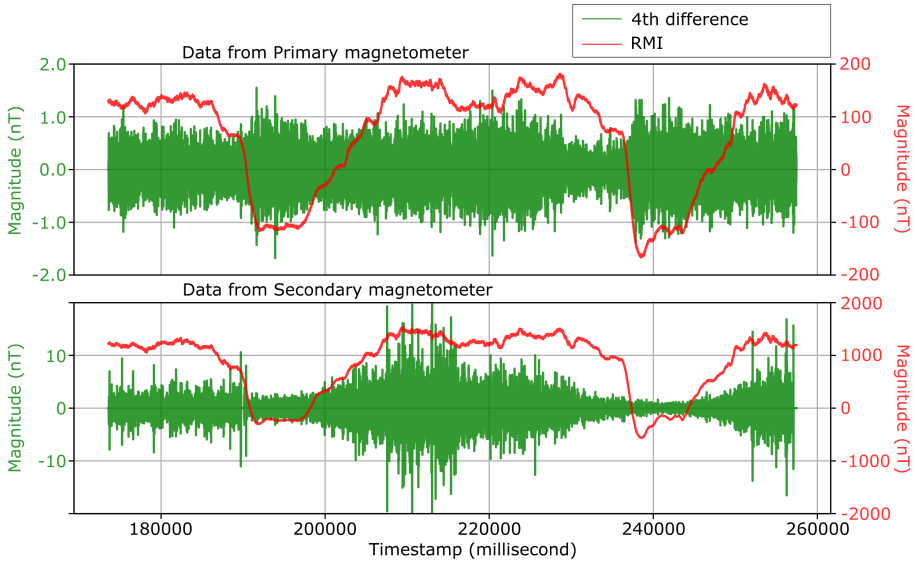


**Figure 9.** Data excerpt of ~~the~~ RMI profiles recorded by the primary and secondary magnetometer and their respective fourth difference while the UAV was flown manually in the multi-rotor mode on 2020.01.13 with d = 20 cm and L =20 cm. The IGRF (50560 nT) has been removed.

~~spiky with magnitudes up to ±1 nT, also higher than the industry standard. Apparently, this increase is directly associated with the platform.~~ in the multi-rotor mode. Nevertheless, in principle, such strong noise can still be reduced distancing the magnetic sensors even farther away from sources of magnetic interference.

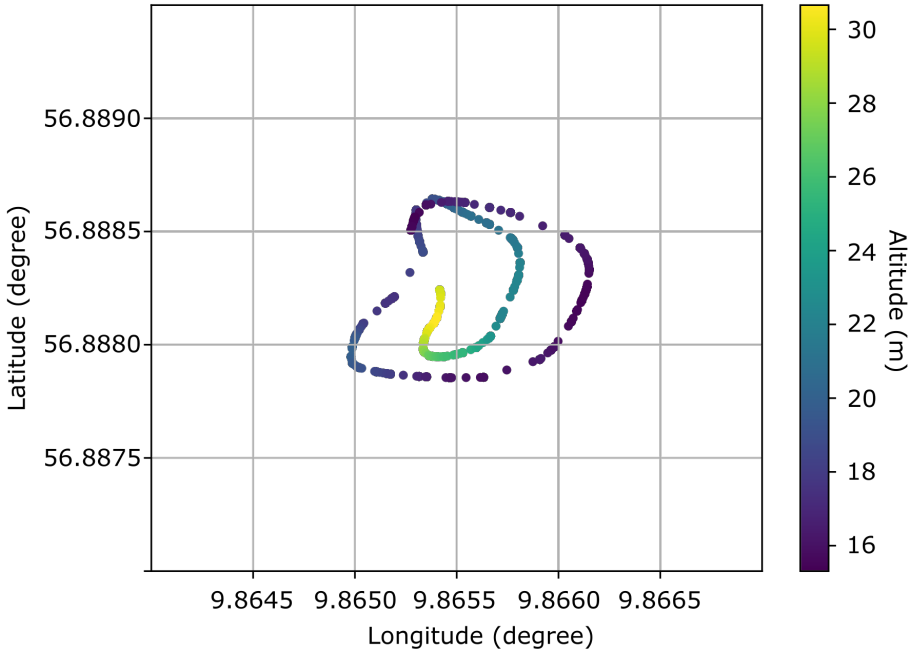


**Figure 10.** The production flight of the data excerpt shown in Fig 9. The altitude indicates the in-flight height above mean sea level.

### 5.3 The second dynamic experiment - fixed-wing mode

Because of the demonstrated strong interference from the UAV in the previous experiment, we increased the distance ($L$) between the secondary magnetometer and the mounting point to ~~$d$ = 20 cm and $L$ =~~ 30 cm to improve the signal-to-noise ratio. ~~In addition, we planned an experiment in the fixed-wing mode to~~ The distance ($d$) between the two magnetometers remained 20 cm. To reduce the dynamic noise observed in the first experiment ~~. Given that the~~ and given that the aforementioned changes may lead to ~~in-flight instability, we required the pilot to fly the UAV manually~~ some instability, the UAV was also flown manually but in the fixed-wing mode for the second experiment. The sampling rate of the QTFMs was 200 Hz~~as well. Similarly, we show residual magnetic intensity~~. The data collected in the standby phase ~~(Fig 11)~~ and then during the fixed-wing flight ~~(Fig~~ are shown in Fig 11, 12, 13, 14 and 15~~)~~.

In comparison with the data gathered in the previous experiment, there is a noticeable increase in the magnitude of the RMI in Fig 11, probably ~~owing to the fact that the amount of~~ because of changes in the direct current flowing in the ~~wires~~cables, the orientation of the ~~wires~~cables, and even the actual distance between the magnetometers and the ~~wires were changed while we were preparing~~ cables while the system in the field ~~. Besides, an extra metal GPS~~ was being prepared. An extra metal GNSS antenna was deployed inside the fuselage to timestamp magnetic recordings during the first experiment, which was solely used at the beginning to synchronize the sensors, after which it was removed to reduce the magnetic interference. Nevertheless, the difference between the actual measurements from the two magnetometers was still surprisingly big, ~~up to~~ around 106 nT~~, leading a longitudinal gradient of 530 nT/m~~. The second experiment was conducted at the same test site as the first one, so the local geomagnetic field should remain roughly constant. Consequently, ~~this strong gradient~~ the big difference between the two magnetic profiles must be somehow introduced by the platform. Interestingly, the fourth difference ~~from~~ of the measurements from the secondary magnetometer is ~~relatively~~ slightly bigger than that of the data from the primary magnetometer ~~, but comparable, both~~ within an envelope of $\pm$0.2 nT. ~~Therefore, since~~ Since the fourth difference of the primary and secondary ~~magnetometer~~ magnetic profiles is comparable in magnitude, it is difficult to say whether the noise originates mainly from the platform ~~itself~~ or cultural noise in the vicinity. ~~However, it~~ It is clear that with the longer boom, the signal-to-noise ratio irrelevant to aircraft maneuvers is improved significantly especially for the secondary magnetometer.

Furthermore, Figure 12 and 13 present the RMI from both magnetometers and current load from the battery monitored by the ~~onboard~~ system in the flight from the take-off to the fixed-wing cruise accompanied by their ~~corresponding~~ respective fourth difference. Take Fig 12 for example - the first part of the RMI (outlined with dark grey box) was collected in the take-off phase (in the multi-rotor mode), whereas the rest was ~~measured~~ recorded in the fixed-wing cruise ~~phase. And the gaps in the plot of the RMI~~ mode. The gaps inside each RMI profile were due to in-flight maneuvers of the UAV somehow rendering the ~~QTFMs falling into dead zones at those moments.~~

~~The two plots of the RMI~~ magnetic field falling into the QTFMs' dead zone. The two RMI profiles in Fig 12 and 13 are ~~two~~ also visually identical, akin to the previous experiment. But the two ~~plots visually look smoother than the data~~ profiles look visually smoother than those collected in the multi-rotor mode. ~~Besides~~Interestingly, a clear correlation ~~is observed~~ between the RMI profiles and the output current from the battery, especially during the take-off phase, ~~but later after~~ is observed. After

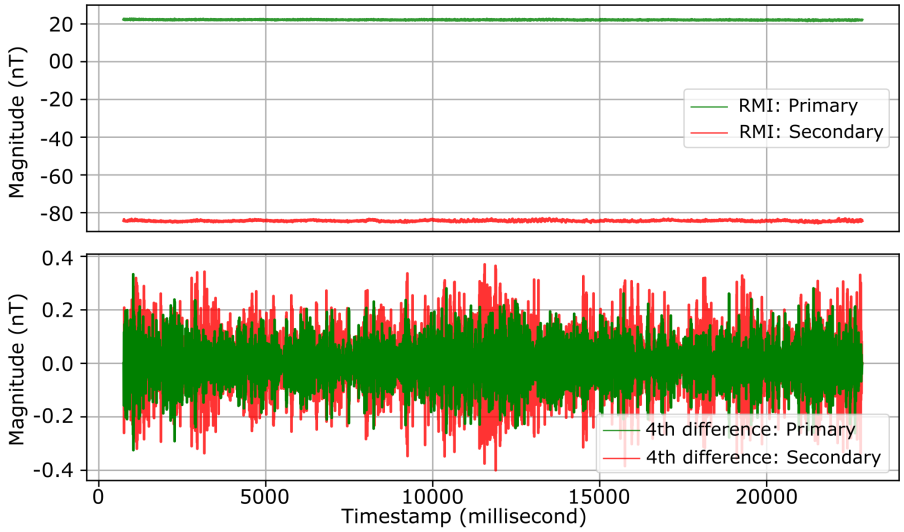


**Figure 11.** Data excerpt of ~~the~~ RMI ~~and the fourth difference~~ profiles recorded by the primary and secondary magnetometer and their respective fourth difference while the UAV was on standby ~~on 2020.03.05~~ with d = 20 cm and L = 30 cm on 2020.03.05. The IGRF (50563 nT) has been removed.

transitioning to fixed-wing mode, there is a clear decrease in the current and the magnetic field~~decreases accordingly~~. The magnitude of the two ~~plots~~ magnetic profiles in Fig 15 are quite comparable before ~~1.583412e12 + 110000 millisecond (epoch time since 1970.01.01)~~170000 milliseconds, but after that moment, the difference in the magnitude increases significantly, ~~five times bigger,~~ which means that the ~~secondary magnetometer is~~ magnetometers are still highly susceptible to the inference from the UAV. ~~Besides, the~~ The plots of the RMI in Fig 15 show a visually clear correlation with the pitch. The fourth difference of the in-flight measurements of the primary magnetometer during the fixed-wing cruise is around $\pm 0.2$ nT (Fig 15), slightly higher than the data collected before the take-off. It is evident that the fixed-wing mode gives less noisy data~~as expected~~.

## 6 Discussion

Based on the static and dynamic experiments, it is obvious that the magnetic interference from the platform is rather ~~complicated~~complex, especially when the platform is in flight. From the static magnetic interference mapping, we have acquired insights into some potential regions on the platform. However, solely measuring static magnetic signature is not sufficient to provide decisive information for the development of an airborne magnetometry system. ~~Therefore, trying to address the complex~~ It seems more practical to understand the interplay between the ~~onboard electronic components is more practical and important, especially~~ dynamic and complex magnetic interference when the platform is properly powered and in operation. For example, the static magnetic signature indicates that the interference at the primary and the secondary magnetometer is minimal and the longitudinal difference is less than 5 nT. ~~Hence,~~ Because during the static magnetic interference measurement, the major interference

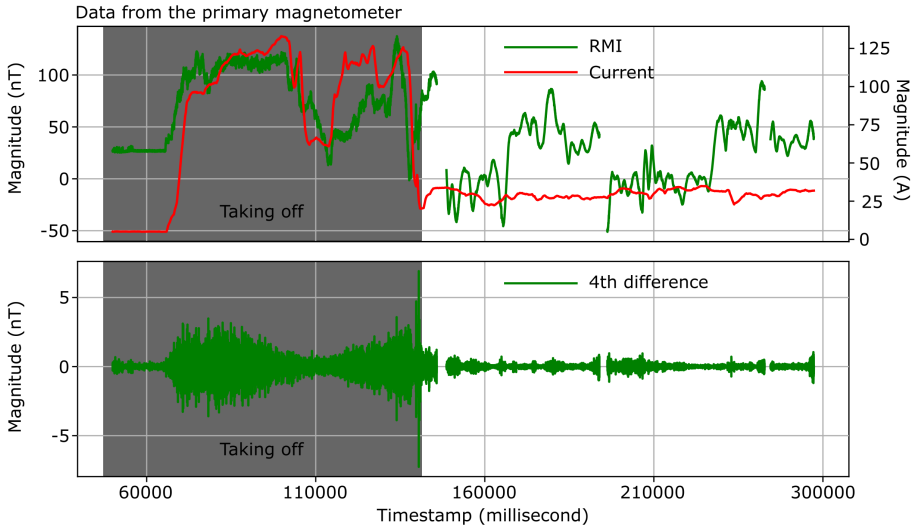


**Figure 12.** Data excerpt of ~~the~~ RMI profile recorded by the primary magnetometer ~~while~~ and its fourth difference, together with the ~~UAV was manually flown in~~ profile of output current from the ~~fixed-wing mode on 2020.03.05~~ battery with d = 20 cm and L = 30 cm. The IGRF (50563 nT) has been removed

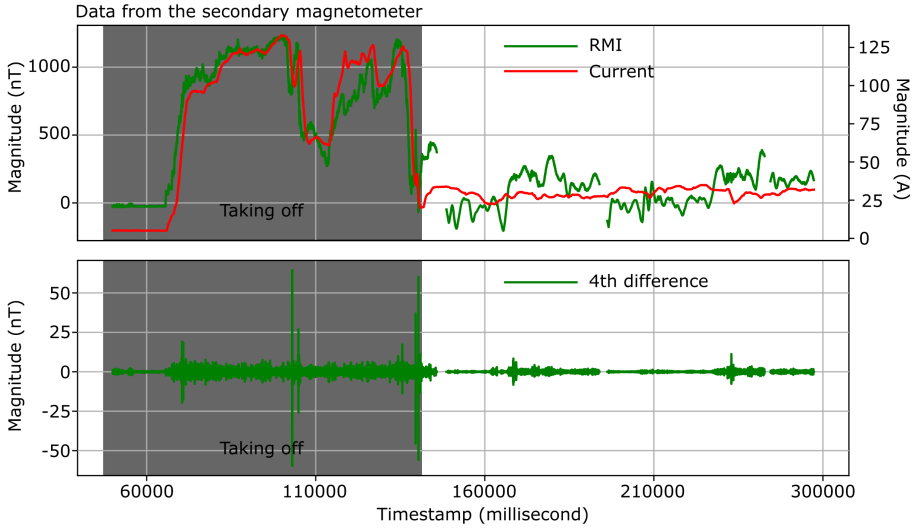


**Figure 13.** Data excerpt of ~~the~~ RMI profile recorded by the secondary magnetometer ~~while~~ and its fourth difference, together with the ~~UAV was manually flown in~~ profile of output current from the ~~fixed-wing mode on 2020.03.05~~ battery with d = 20 cm and L = 30 cm. The IGRF (50563 nT) has been removed

is due to the permanent magnets of the electric ~~actuators~~ servomotors and electric motors. ~~However, while~~ Once the platform is powered and flying in operation, ~~the~~ magnetic interference increases significantly. The reason for the increase can

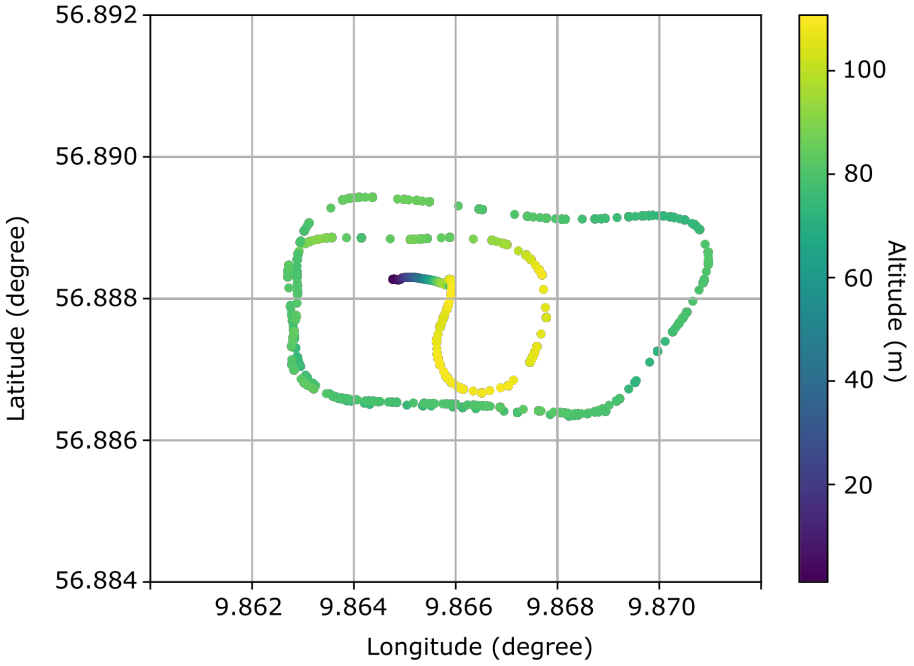


**Figure 14.** The production flight of the data excerpt shown in Fig 12 and 13. The altitude indicates the in-flight height above mean sea level.

be magnetic leakage of the electric ~~actuators~~ servomotors and electric motors, the magnetic field generated by dynamically-varying current flowing from the battery to flight controller, and the magnetic interference due to eddy current in the airframe. ~~Interestingly~~Surprisingly, in comparison with the first dynamic experiment, the magnetic interference ~~has also changed considerably in the~~ observed in the standby phase in the second dynamic experiment ~~in the standby phase~~has also changed considerably. In principle, the longer boom provides increased distance to sources of interference leading to a stronger attenuation of interference from the platform, but ~~on the contrary~~in the experiments, the longitudinal gradient between the primary and the secondary magnetometers increased by ten times than that in the first dynamic experiment. The first variable between the two dynamic tests is power consumption because the platform consumes way more power in the multi-rotor mode than in the fixed-wing mode, which leads to strong current in the ~~wires~~cables. The second variable is the layout of the components inside the fuselage ~~on-site~~ such as the orientation of the ~~wires~~ current-carrying cables connecting the battery with the flight controller. ~~Besides, we also find out that the wires~~ The current-carrying cables are quite soft ~~so that the wires can actually move freely inside the fuselage due to inertia once the~~ and can dangle with the aircraft's attitude ~~or speed changes and also it is clear that the transversal dimension of the fuselage on the platform is way smaller than the longitudinal dimension (see Fig 4), so once the wires start moving, there is more space for the wires to move~~ along the longitudinal axis of the ~~UAV than that along other axes. It can explain why the RMI in Fig 15 shows~~ fuselage, which led to such a stronger correlation with the pitch (Fig 16) other than the superimposition effects of all the maneuvers~~, even though the roll changed more violently than the pitch (Fig 15 and 16)~~.

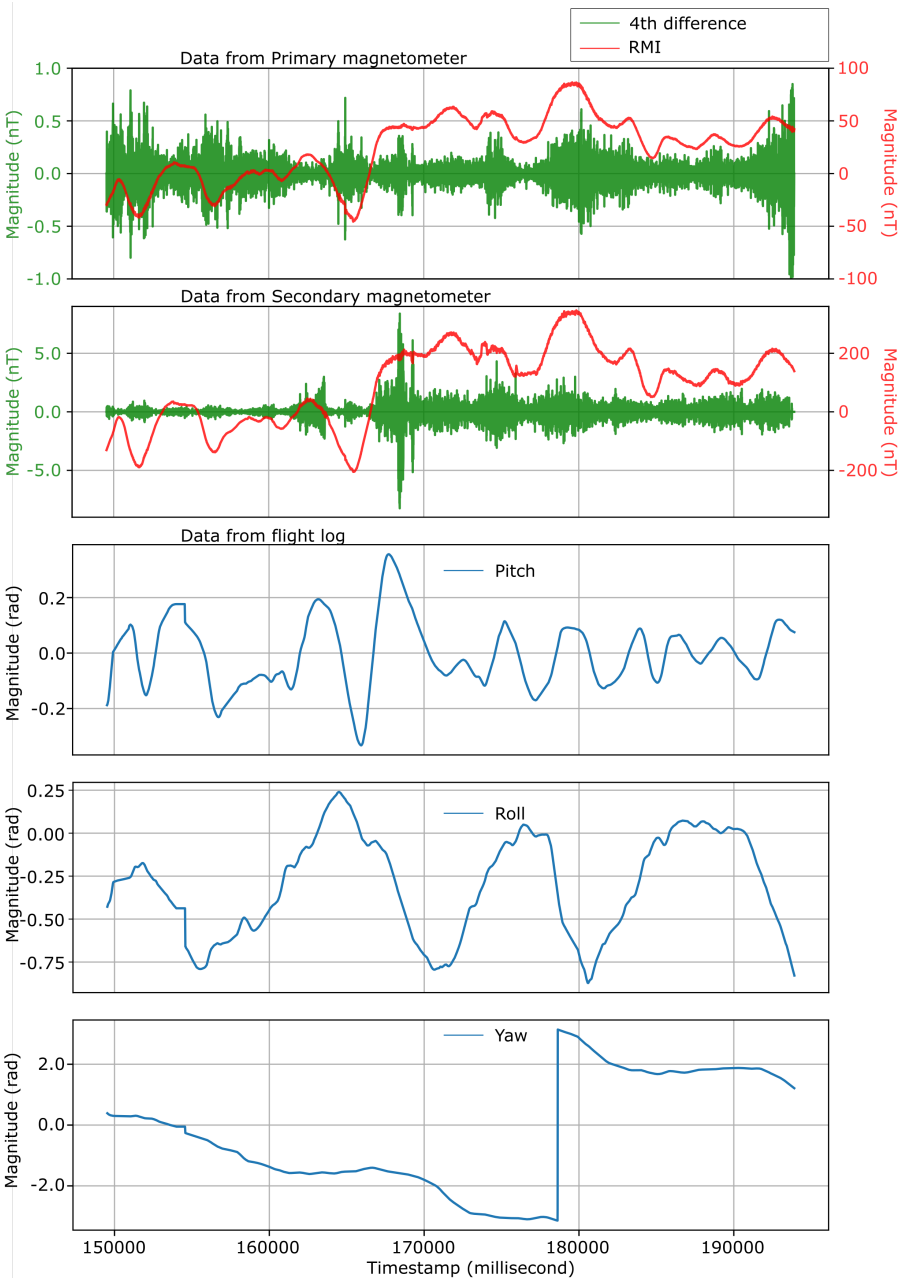


**Figure 15.** The RMI of the second segment from left to right in Fig 12 and 13 and the corresponding attitude from flight log.

Regarding the issues ~~, we have~~ that have been discovered, we ~~first agreed~~ will try to further increase the distance between the magnetometers and the platform without compromising the flight stability, because the noise envelop at the moment is too high to meet the industry standard for mineral exploration. ~~Second, the wires~~ Secondly, the cables connecting the battery ~~and~~

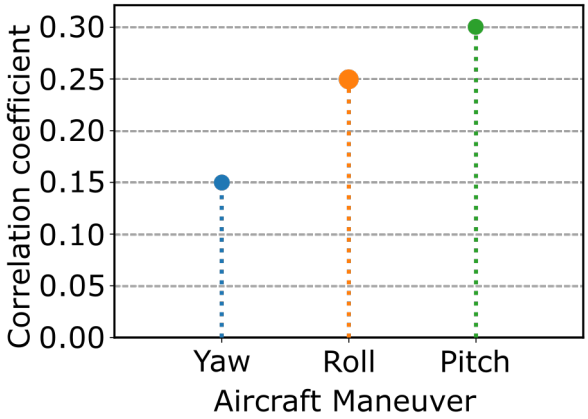


**Figure 16.** Correlation coefficient of the RMI and aircraft maneuvers.

with the flight controller should be properly placed and shielded to further reduce the interference. ~~Therefore, the next step is to consider how and where the components inside the fuselage should be placed.~~

## 7 Conclusions

We presented a static experiment, and based on the assessment of the results of the static experiment, we proposed a front-boom mounting system, of which stability is supported by our aerodynamic simulations. Later we conducted two dynamic experiments to ~~understand~~ assess in-flight noise in operation. The results are insightful because surprisingly the strongest interference ~~comes from the wires~~ originates from the cables connecting the Li-Po battery to the flight controller. As a consequence, we propose to further increase the distance between the magnetic sensors and the UAV~~again. Besides, we will try to shield the magnetic interference coming for the wires and also try to put the cable in the back of the fuselage to further keep the interference away from the magnetic field observation system~~. Additional noise reduction measures include shielding the cables causing strong magnetic interference and relocating the UAV's wiring harness.

*Data availability.* The data used in the manuscript are available from the corresponding author, upon reasonable request.

*Author contributions.* The authors contributed equally to this work.

*Competing interests.* The authors declare that there are no competing interests regarding the publication of this paper.

*Acknowledgements.* The work is funded by the European Institute of Technology & Innovation – Raw Materials (EIT-RM). We would also like to thank Sky-Watch A/S for their support.

## References


A. D. P. Juliani, D. P. Gonzaga, and J. R. B. A. Monteiro: Magnetic field analysis of a brushless DC motor, in: 2008 18th International Conference on Electrical Machines, pp. 1–6, https://doi.org/10.1109/ICELMACH.2008.4800146, 2008.

Aminzadeh, F. and Dasgupta, S. N.: Chapter 3 - Fundamentals of Petroleum Geophysics, in: Geophysics for Petroleum Engineers, edited by Aminzadeh, F. and Dasgupta, S. N., vol. 60 of *Developments in Petroleum Science*, pp. 37 – 92, Elsevier, https://doi.org/10.1016/B978-0-444-50662-7.00003-2, 2013.

Chen, L., Wu, P., Zhu, W., Feng, Y., and Fang, G.: A novel strategy for improving the aeromagnetic compensation performance of helicopters, Sensors, 18, 1846, https://doi.org/10.3390/s18061846, 2018.

Chung, D. D.: Functional Materials: Electrical, Dielectric, Electromagnetic, Optical and Magnetic Applications:(with Companion Solution Manual), vol. 2, World scientific, https://doi.org/10.1142/7447, 2010.

Council, N. R.: Airborne Geophysics and Precise Positioning: Scientific Issues and Future Directions, The National Academies Press, Washington, DC, https://doi.org/10.17226/4807, 1995.

Coyle, M., Dumont, R., Keating, P., Kiss, F., and Miles, W.: Geological Survey of Canada aeromagnetic surveys: Design, quality assurance, and data dissemination, Geological Survey of Canada, https://doi.org/10.4095/295088, 2014.

Cunningham, M.: Aeromagnetic surveying with unmanned aircraft systems, Ph.D. thesis, Carleton University, https://doi.org/10.22215/etd/2016-11270, 2016.

Eppelbaum, L. and Mishne, A.: Unmanned Airborne Magnetic and VLF Investigations: Effective Geophysical Methodology for the Near Future, Positioning, 2011, https://doi.org/10.4236/pos.2011.23012, 2011.

Eppelbaum, L. V.: Study of magnetic anomalies over archaeological targets in urban environments, Physics and Chemistry of the Earth, Parts A/B/C, 36, 1318–1330, https://doi.org/10.1016/j.pce.2011.02.005, 2011.

Eppelbaum, L. V.: Quantitative interpretation of magnetic anomalies from bodies approximated by thick bed models in complex environments, Environmental Earth Sciences, 74, 5971–5988, https://doi.org/10.1007/s12665-015-4622-1, 2015.

Fairhead, J. D.: 12 - Regional tectonics and basin formation: The role of potential field studies, in: Regional Geology and Tectonics: Principles of Geologic Analysis, edited by Roberts, D. and Bally, A., pp. 330 – 341, Elsevier, Amsterdam, https://doi.org/10.1016/B978-0-444-53042-4.00012-1, 2012.

Forrester, R. W.: Magnetic signature control strategies for an unmanned aircraft system, Ph.D. thesis, Carleton University, https://doi.org/10.22215/etd/2011-07308, 2011.

Håkansson, E. and Surlyk, F.: Encyclopedia of European and Asian Regional Geology, chap. Oil and gas Denmark, pp. 183–192, Springer Netherlands, Dordrecht, https://doi.org/10.1007/1-4020-4495-X_25, 1997.

Haldar, S. K.: Chapter 6 - Exploration Geophysics, in: Mineral Exploration (Second Edition), edited by Haldar, S. K., pp. 103 – 122, Elsevier, second edition edn., https://doi.org/10.1016/B978-0-12-814022-2.00006-X, 2018.

Hansen, C. R. D.: Magnetic signature characterization of a fixed-wing vertical take-off and landing (VTOL) unmanned aerial vehicle (UAV), Ph.D. thesis, 2018.

Hinze, W. J., Von Frese, R. R., and Saad, A. H.: Gravity and magnetic exploration: Principles, practices, and applications, Cambridge University Press, https://doi.org/10.1017/CBO9780511843129, 2013.

Kaneko, T., Koyama, T., Yasuda, A., Takeo, M., Yanagisawa, T., Kajiwara, K., and Honda, Y.: Low-altitude remote sensing of volcanoes using an unmanned autonomous helicopter: an example of aeromagnetic observation at Izu-Oshima volcano, Japan, International Journal of Remote Sensing, 32, 1491–1504, https://doi.org/10.1080/01431160903559770, 2011.

Kolster, M. and Døssing, A.: Scalar magnetic difference inversion applied to UAV-based UXO detection, Geophysical Journal International, under review, 2020.

Kruse, S.: 3.5 Near-Surface Geophysics in Geomorphology, in: Treatise on Geomorphology, edited by Shroder, J. F., pp. 103 – 129, Academic Press, San Diego, https://doi.org/10.1016/B978-0-12-374739-6.00047-6, 2013.

Malehmir, A., Dynesius, L., Paulusson, K., Paulusson, A., Johansson, H., Bastani, M., Wedmark, M., and Marsden, P.: The potential of rotary-wing UAV-based magnetic surveys for mineral exploration: A case study from central Sweden, The Leading Edge, 36, 552–557, https://doi.org/10.1190/tle36070552.1, 2017.

Mu, Y., Zhang, X., Xie, W., and Zheng, Y.: Automatic Detection of Near-Surface Targets for Unmanned Aerial Vehicle (UAV) Magnetic Survey, Remote Sensing, 12, 452, https://doi.org/10.3390/rs12030452, 2020.

Nabighian, M. N., Grauch, V., Hansen, R., LaFehr, T., Li, Y., Peirce, J., Phillips, J., and Ruder, M.: The historical development of the magnetic method in exploration, Geophysics, 70, 33ND–61ND, https://doi.org/10.1190/1.2133784, 2005.

Nikulin, A. and de Smet, T. S.: A UAV-based magnetic survey method to detect and identify orphaned oil and gas wells, The Leading Edge, 38, 447–452, https://doi.org/10.1190/tle38060447.1, 2019.

Parshin, A. V., Morozov, V. A., Blinov, A. V., Kosterev, A. N., and Budyak, A. E.: Low-altitude geophysical magnetic prospecting based on multirotor UAV as a promising replacement for traditional ground survey, Geo-spatial information science, 21, 67–74, https://doi.org/10.1080/10095020.2017.1420508, 2018.

Parvar, K., Braun, A., Layton-Matthews, D., and Burns, M.: UAV magnetometry for chromite exploration in the Samail ophiolite sequence, Oman, Journal of Unmanned Vehicle Systems, 6, 57–69, https://doi.org/10.1139/juvs-2017-0015, 2017.

Perry, A. R., Czipott, P. V., and Walsh, D. O.: Rapid area coverage for unexploded ordnance using UAVs incorporating magnetic sensors, in: Battlespace Digitization and Network-Centric Warfare II, vol. 4741, pp. 262–269, International Society for Optics and Photonics, https://doi.org/10.1117/12.478720, 2002.

Reeves, C.: Aeromagnetic surveys: principles, practice & interpretation, Geosoft, 2005.

Reeves, C., Reford, S., Milligan, P., and Gubins, A.: Airborne geophysics: old methods, new images, in: Proceedings of exploration, vol. 97, pp. 13–30, https://doi.org/10.1017/CBO9780511549816, 1997.

Reid, A.: Aeromagnetic survey design, Geophysics, 45, 973–976, https://doi.org/10.1190/1.1441102, 1980.

Richard L., S.: The analysis of eddy currents, Oxford University Press, 1974.

Samson, C., Straznicky, P., Laliberté, J., Caron, R., Ferguson, S., and Archer, R.: Designing and building an unmanned aircraft system for aeromagnetic surveying, in: SEG Technical Program Expanded Abstracts 2010, pp. 1167–1171, Society of Exploration Geophysicists, https://doi.org/10.1190/1.3513051, 2010.

Sterligov, B. and Cherkasov, S.: Reducing Magnetic Noise of an Unmanned Aerial Vehicle for High-Quality Magnetic Surveys, https://doi.org/10.1155/2016/4098275, 2016.

Sterligov, B., Cherkasov, S., Kapshtan, D., and Kurmaeva, V.: An experimental aeromagnetic survey using a rubidium vapor magnetometer attached to the rotary-wings unmanned aerial vehicle, First Break, 36, 39–45, https://doi.org/10.3997/1365-2397.2017023, 2018.

Tuck, L.: Characterization and compensation of magnetic interference resulting from unmanned aircraft systems, Ph.D. thesis, Carleton University, 2019.

Tuck, L., Samson, C., Laliberté, J., Wells, M., and Bélanger, F.: Magnetic interference testing method for an electric fixed-wing unmanned aircraft system (UAS), Journal of Unmanned Vehicle Systems, 6, 177–194, https://doi.org/10.1139/juvs-2018-0006, 2018.

Turner, G., Rasson, J., and Reeves, C.: 5.04 - Observation and Measurement Techniques, in: Treatise on Geophysics (Second Edition), edited by Schubert, G., pp. 91 – 135, Elsevier, Oxford, second edition edn., https://doi.org/10.1016/B978-0-444-53802-4.00098-1, 2015.

Wood, A., Cook, I., Doyle, B., Cunningham, M., and Samson, C.: Experimental aeromagnetic survey using an unmanned air system, The Leading Edge, 35, 270–273, https://doi.org/10.1190/tle35030270.1, 2016.

Zhou, W.: Encyclopedia of Engineering Geology, chap. Aeromagnetic Survey, pp. 13–18, Springer International Publishing, Cham, https://doi.org/10.1007/978-3-319-73568-9_8, 10.1007/978-3-319-73568-9_8, 2018.